

Enhanced photoluminescence in air-suspended carbon nanotubes by oxygen doping

Jihan Chen,¹ Rohan Dhall,¹ Bingya Hou,¹ Sisi Yang,² Bo Wang,² Daejing Kang,³ and Stephen B. Cronin^{1,2}

¹Ming Hsieh Department of Electrical Engineering, University of Southern California, Los Angeles, California 90089, USA

²Department of Physics and Astronomy, University of Southern California, Los Angeles, California 90089, USA

³Department of Mechatronics Engineering, Korea Polytechnic University, Shiheung-shi, Gyunggi-do 15073, South Korea

(Received 22 June 2016; accepted 25 September 2016; published online 12 October 2016)

We report photoluminescence (PL) imaging and spectroscopy of air-suspended carbon nanotubes (CNTs) before and after exposure to a brief (20 s) UV/ozone treatment. These spectra show enhanced PL intensities in 10 out of 11 nanotubes that were measured, by as much as 5-fold. This enhancement in the luminescence efficiency is caused by oxygen defects which trap excitons. We also observe an average 3-fold increase in the *D*-band Raman intensity further indicating the creation of defects. Previous demonstrations of oxygen doping have been carried out on surfactant-coated carbon nanotubes dissolved in solution, thus requiring substantial longer ozone/UV exposure times (~15 h). Here, the ozone treatment is more efficient because of the surface exposure of the air-suspended CNTs. In addition to enhanced PL intensities, we observe narrowing of the emission linewidth by 3–10 nm. This ability to control and engineer defects in CNTs is important for realizing several optoelectronic applications such as light-emitting diodes and single photon sources. *Published by AIP Publishing.* [<http://dx.doi.org/10.1063/1.4964461>]

Over the past few years, oxygen doping of carbon nanotubes (CNTs) through ozonolysis has been shown to produce localized exciton states that exhibit enhanced photoluminescence (PL) intensities (~20×), long photoluminescence lifetimes (>1 ns), and promising photon antibunching signatures for single photon emission, even at room temperature.^{1–7} In the work of Htoon *et al.*,¹ surfactant-coated carbon nanotubes suspensions were mixed with ozone saturated water and exposed to UV light for 17 h. In their experiments, not only deep trap emission peak for oxygen-doped nanotubes in the 1.06–1.15 eV PL spectral range were observed but also multiple sharp asymmetric emission peaks were reported at energies 50–300 meV redshifted from the E_{11} bright exciton peak. In the work of Weisman *et al.*,³ surfactant-coated carbon nanotubes were exposed to ozone and white light for up to 16 h. They found that the oxygen-doped single-walled carbon nanotubes (SWCNTs) are much easier to detect than pristine SWCNTs because they give stronger near-infrared emission. This work also showed distinct near-infrared fluorescence at wavelengths 10%–15% longer than displayed in pristine semiconducting SWCNTs. In the work of Violla *et al.*, the PL spectra of nanotubes show the emergence of sharp peaks at low temperatures corresponding to localized excitons coupling to phonons.⁴ The work of Hofmann *et al.* showed that, at low temperature, excitons in suspended nanotubes become localized around defect sites and exhibit long-lived luminescence emission, greater than 3 ns.⁵ Similar results can also be found in the work of Sarpkaya *et al.*, who reported PL lifetimes up to 18 ns from localized excitons.⁶ In the work of Ma *et al.*, oxygen dopant states were controllably introduced, leading to extend lifetimes and single photon emission even at room temperature.⁷ While

these previous results are exciting and demonstrate the ability to control defects in CNTs for improved light emission, the surfactant-coated geometry is not ideal for device fabrication. The emission wavelength of these previous studies remained close to or below 1000 nm. In the work presented here, we study enhanced emission out to the 1550 nm wavelength range, which is compatible with fiber optic telecommunications.

Here, we apply a UV/ozone treatment to air-suspended carbon nanotubes. Because of the exposed surface of the CNTs, sufficient O-doping for enhanced PL is achieved in just 20 s, 3 orders of magnitude more rapidly than previous attempts on surfactant-coated CNTs dissolved in solution.^{8–14} Since ozone can damage carbon nanotubes,^{15,16} care was taken to minimize the exposure required to produce localized excitons. Raman spectra are also collected before and after the UV/ozone treatment in order to further characterize the defect creation process.^{12,17,18}

In this work, $2\ \mu\text{m} \times 2\ \mu\text{m}$ pillars are etched $8\ \mu\text{m}$ deep in a quartz substrate using a Cl-based reactive ion etch plasma, as shown in Fig. 1. 1 nm of Fe is deposited on the pillars to serve as a catalyst for the nanotube growth. Carbon nanotubes are grown by chemical vapor deposition (CVD) at 825 °C using ethanol as the carbon feedstock,^{19,20} resulting in CNTs suspended across adjacent pillars, as shown in Figure 1(d). PL images were taken using a defocused 785 nm laser in conjunction with a thermoelectrically cooled InGaAs camera (Xenics, Inc.) with a 5 s integration time. The ozone treatment was carried out in a UV/ozone cleaner (ProCleaner, BioForce, Inc.) using ambient air at 1 atm for 20 s. This UV/ozone cleaner uses a 10.15 W mercury, non-phosphorus coated quartz lamp (~4.6 mW/cm² at the sample surface). The lamp spectrum is

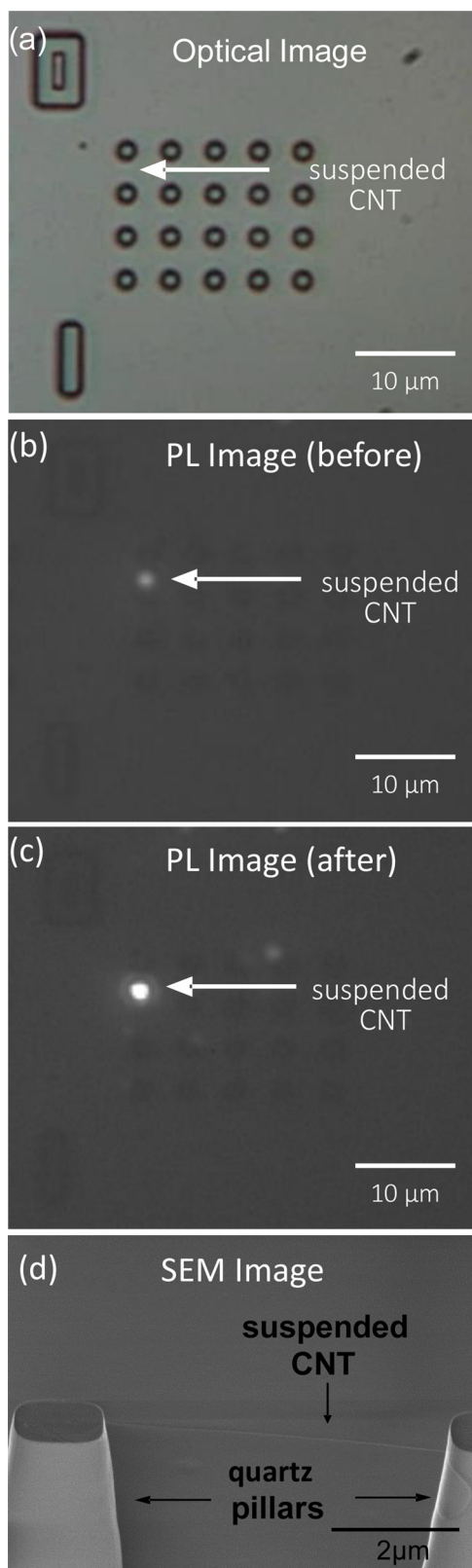


FIG. 1. (a) Optical microscope image of quartz pillar arrays. Photoluminescence image of suspended CNT (b) before and (c) after UV/ozone treatment. (d) SEM image of CNT suspended on top of the pillars.

mostly concentrated in the 180 nm–440 nm range peaking at 254 nm. Raman and PL spectra were collected using a Renishaw *InVia* micro-spectrometer equipped with both silicon and InGaAs detector arrays. Scanning electron microscope (SEM) images (Figure 1(d)) were taken after all optical

characterization, in order to avoid quenching the CNT photoluminescence.

An optical microscope image of a 4×5 array of quartz pillars is shown in Figure 1(a). Figure 1(b) shows a PL image taken from the same region of this sample before ozone treatment. A faint line can be seen connecting two adjacent pillars, corresponding to PL emission from a suspended CNT. Figure 1(c) shows a PL image of the same sample after ozone treatment, exhibiting a much brighter line, indicating substantial enhancement in the PL emission. In addition to the bright line in this image, several new bright spots appear originating from other CNTs that were previously too dim to see. Figure 1(d) shows an SEM image of the suspended CNT connecting two adjacent quartz pillars.

Figure 2 shows the Raman and PL spectra of the suspended CNT shown in Figure 1. A normalized PL spectrum is also included in [supplementary material](#) as Figure S1. A sharp radial breathing mode (RBM) can be seen at 150 cm^{-1} (FWHM = 10 cm^{-1}). While the frequency of this mode remains essentially unchanged after the ozone treatment, we observe a substantial linewidth broadening after UV/ozone treatment, most likely due to sample inhomogeneity. The PL spectra exhibit a sharp peak centered at 1530 nm (FWHM = 28 nm). The linewidth was fitted without including the shoulder at 1510 and 1560 nm, which are possibly due to phonon sidebands. In previous literature, similar spectral wings have been attributed to phonon sidebands emerging at low temperature, but were not observed at room temperature.^{4,21} This peak can be seen to increase in intensity by a factor of $5.1 \times$, in addition to a linewidth

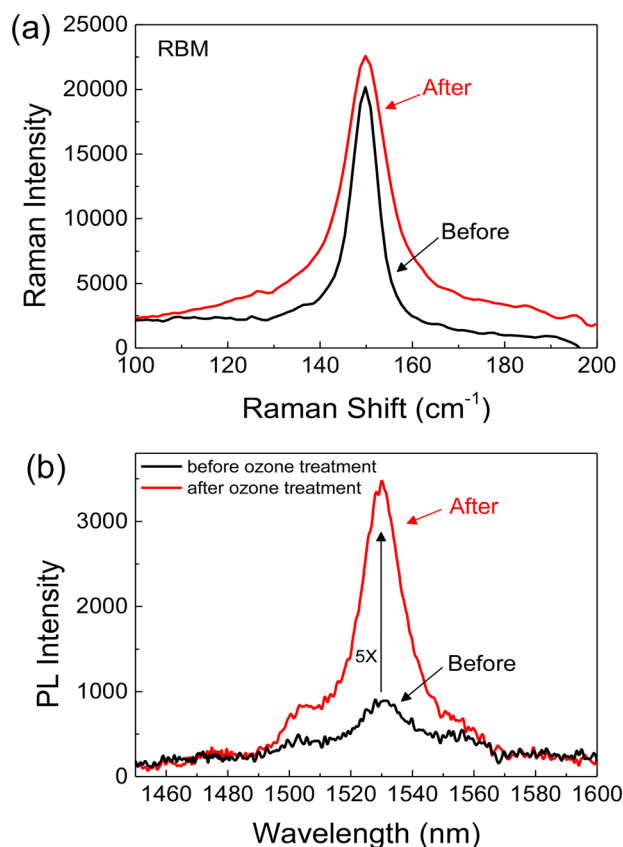


FIG. 2. (a) Radial breathing mode (RBM) Raman spectra and (b) PL spectra of CNT before (black) and after (red) exposure to the UV/ozone treatment.

TABLE I. The PL intensity, linewidth, and center wavelength for 10 suspended CNT samples before and after UV/ozone treatment. The PL intensity enhancement and linewidth narrowing can be observed after UV/ozone treatment, which are due to the introduction of oxygen atoms.

Sample	RBM (cm^{-1})	PL intensity peak height		PL linewidth (nm)		PL center wavelength (nm)	
		Before	After	Before	After	Before	After
1	150	3413	8663	23.1	14.1	1508	1504
2	151	1123	3631	21.4	12.7	1424	1422
3	187	628	3211	28.8	18.2	1530	1530
4	132	449	2189	28.6	18.7	1528	1530
5	148	1553	6735	16.6	11.8	1476	1473
6	238	3619	17148	14.0	10.2	1287	1284
7	227	2606	8180	8.5	11.7	1265	1268
8	201	3737	8776	19.0	13.5	1476	1472
9	203	3747	7458	15.2	11.2	1352	1352
10	202	3634	8448	11.1	14.5	1420	1420
Average	179	2451	7444	18.6	13.6	1427	1425

narrowing of 10 nm after UV/ozone treatment. The PL spectra peak position remains nearly unchanged after UV/ozone treatment. We believe that the PL intensity enhancement shown in Fig. 2(b) originates from the introduction of oxygen atoms as dopants in our suspended CNTs. Those oxygen atoms create perturbed regions in the CNT that trap excitons, and result in more efficient radiative recombination. Thus, the PL intensity enhancement and linewidth narrowing can be observed after UV/ozone treatment. Unlike the previous reports in the literature, there are no new redshifted features in the PL spectra. Enhanced photoluminescence emission was observed in 10 out of a total of 11 individual air-suspended carbon nanotubes after a 20-s UV/ozone treatment. These results are summarized in Table I. Here, an average increase in PL intensity of $3\times$ is observed as well as a linewidth narrowing from an average of 18.6 nm–13.6 nm after UV/ozone exposure. While most of the nanotubes show linewidth narrowing, samples 7 and 10 show a linewidth broadening, which could be due to the presence of many defects causing inhomogeneous broadening. The photoluminescence emission from the nanotubes in this study lie in the wavelength range from 1265 to 1530 nm. This range is largely determined by the finite diameter distribution and the fixed excitation laser wavelength (785 nm), which samples only a small portion of the

Kataura space. In order to extend these wavelengths to 1550 nm, different diameters should be selected, and a longer excitation wavelength should be used. Typically, trapped excitons are lower in energy by several $k_B T$ with respect to free exciton states. However, here, we do not observe any systematic redshift in our spectra. One possible explanation for this is that the excitons are getting imprisoning between two reflecting O-defects. Another possible explanation is that the O-plasma treatment is simply cleaning the surface of these nanotubes (i.e., removing non-radiative recombination centers), thus not producing a redshift.

The *D*- and *G*-band Raman spectra taken before and after UV/ozone treatment are plotted in Figure 3. Here, we see a 3-fold increase in the *D*-band Raman intensity, corresponding to the introduction of defects, while the intensity of the *G*-band does not change after UV/ozone treatment. Table II lists a summary of changes observed in the *D*-band Raman intensity and *G*-band linewidth after UV/ozone treatment. While substantial changes in the *G*-band linewidth (both broadening and narrowing) are observed, no symmetric shift is observed in the ten samples measured in this study. All ten

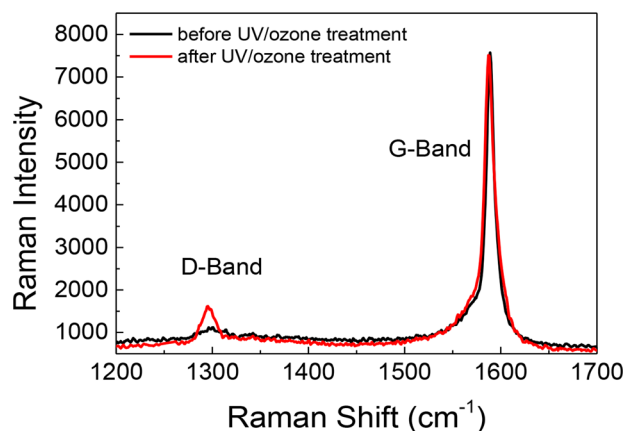


FIG. 3. *D*- and *G*-band Raman spectra of CNT before (black) and after (red) exposure to the UV/ozone treatment.

TABLE II. The *D*-band intensity and *G*-band linewidth of 10 suspended CNT samples before and after UV/ozone treatment. After UV/ozone treatment, a substantial increase in the *D*-band Raman intensity is observed, while the intensity of the *G*-band does not change indicating the introduction of defects.

Sample	<i>D</i> -band intensity		<i>G</i> -band linewidth (cm^{-1})	
	Before	After	Before	After
1	1399	5911	8.4	12.5
2	334	975	10.5	14.7
3	3572	7118	8	10.4
4	3045	7018	9.8	7.5
5	732	2361	9.6	10.5
6	1167	8255	25.7	13
7	576	1288	10.8	13.2
8	854	2658	11	14.5
9	1307	3577	10.4	13.6
10	750	2479	12.3	15
Average	1374	4164	11.7	12

of these nanotubes, however, showed a substantial increase in the *D*-band Raman intensity.

We also performed longer UV/ozone exposures to the photoluminescent pristine CNT for 2 min. After the 2-min UV/ozone exposure (Figure S2 of the [supplementary material](#)), all of the bright spots disappear. Previous demonstrations of oxygen doping have been carried out on surfactant-coated carbon nanotubes dissolved in solution, thus requiring substantial longer ozone/UV exposure times (~ 15 h). Here, the ozone treatment is more efficient because the surface is exposed in these air-suspended CNTs. Therefore, there is an inherent limitation in the UV/ozone treatment of these air-suspended nanotubes. Once a substantial amount of defects are formed, these delicate hanging structures simply collapse, which quenches their photoluminescence. As such, it is unlikely that the high densities of O-defects previously obtained in surfactant coated nanotubes can be achieved using this approach.

In summary, we demonstrate a reliable and scalable method using a UV/ozone treatment to enhance the photoluminescence intensity of air-suspended carbon nanotubes. Here, a 20-s UV/ozone exposure gives enhanced PL intensities by up to a factor of $5\times$. This is considerably more rapid than oxygen doping on surfactant-coated carbon nanotubes dissolved in solution reported in previous literature. The enhanced photoluminescence originates from oxygen defects that locally trap excitons, increasing their radiative recombination efficiency. This UV/ozone treatment also results in a 3-fold increase in the *D*-to-*G* band Raman intensity ratio, further corroborating the creation of defects. The ability to control and engineer defects in CNTs is important for realizing several optoelectronic applications such as light-emitting diodes and single photon sources.

See [supplementary material](#) for normalized PL spectra of carbon nanotubes before and after 20 s UV/ozone exposures and PL images of carbon nanotubes before and after 2 min UV/ozone exposures.

This research was supported by the Department of Energy DOE Award No. DE-FG02-07ER46376 (J.C.) and NSF Award No. 1402906 (S.Y.). We also gratefully acknowledge the support of Karen Trentelman and Catherine Patterson at The Getty Center for use of their InGaAs detector and Dr. Brutchey at USC for the UV/ozone generator.

¹X. Ma, L. Adamska, H. Yamaguchi, S. E. Yalcin, S. Tretiak, S. K. Doorn, and H. Htoon, "Electronic structure and chemical nature of oxygen dopant states in carbon nanotubes," *ACS Nano* **8**, 10782–10789 (2014).

²Y. Miyauchi, M. Iwamura, S. Mouri, T. Kawazoe, M. Ohtsu, and K. Matsuda, "Brightening of excitons in carbon nanotubes on dimensionality modification," *Nat. Photonics* **7**, 715–719 (2013).

- ³S. Ghosh, S. M. Bachilo, R. A. Simonette, K. M. Beckingham, and R. B. Weisman, "Oxygen doping modifies near-infrared band gaps in fluorescent single-walled carbon nanotubes," *Science* **330**, 1656–1659 (2010).
- ⁴F. Vialla, Y. Chassagneux, R. Ferreira, C. Roquelet, C. Diederichs, G. Cassabois, Ph. Roussignol, J. S. Lauret, and C. Voisin, "Unifying the low-temperature photoluminescence spectra of carbon nanotubes: The role of acoustic phonon confinement," *Phys. Rev. Lett.* **113**, 057402 (2014).
- ⁵M. S. Hofmann, J. T. Glückert, J. Noé, C. Bourjau, R. Dehmel, and A. Högele, "Bright, long-lived and coherent excitons in carbon nanotube quantum dots," *Nat. Nanotechnol.* **8**, 502–505 (2013).
- ⁶I. Sarpkaya, Z. Zhang, W. W. Newman, X. Wang, J. Hone, C. W. Wong, and S. Strauf, "Prolonged spontaneous emission and dephasing of localized excitons in air-bridged carbon nanotubes," *Nat. Commun.* **4**, 2152 (2013).
- ⁷X. D. Ma, N. F. Hartmann, J. K. S. Baldwin, S. K. Doorn, and H. Htoon, "Room-temperature single-photon generation from solitary dopants of carbon nanotubes," *Nat. Nanotechnol.* **10**, 671–675 (2015).
- ⁸K. Iakoubovskii, N. Minami, Y. Kim, K. Miyashita, S. Kazaoui, and B. Nalini, "Midgap luminescence centers in single-wall carbon nanotubes created by ultraviolet illumination," *Appl. Phys. Lett.* **89**, 173108 (2006).
- ⁹L. Cai, J. L. Bahr, Y. Yao, and J. M. Tour, "Ozonation of single-walled carbon nanotubes and their assemblies on rigid self-assembled monolayers," *Chem. Mater.* **14**, 4235–4241 (2002).
- ¹⁰S. Banerjee and S. S. Wong, "Rational sidewall functionalization and purification of single-walled carbon nanotubes by solution-phase ozonolysis," *J. Phys. Chem. B* **106**, 12144–12151 (2002).
- ¹¹M. Li, M. Boggs, T. P. Beebe, and C. P. Huang, "Oxidation of single-walled carbon nanotubes in dilute aqueous solutions by ozone as affected by ultrasound," *Carbon* **46**, 466–475 (2008).
- ¹²D. Ogrin, J. Chattopadhyay, A. K. Sadana, W. E. Billups, and A. R. Barron, "Epoxidation and deoxygenation of single-walled carbon nanotubes: Quantification of epoxide defects," *J. Am. Chem. Soc.* **128**, 11322–11323 (2006).
- ¹³M. L. Sham and J. K. Kim, "Surface functionalities of multi-wall carbon nanotubes after UV/Ozone and TETA treatments," *Carbon* **44**, 768–777 (2006).
- ¹⁴A. I. Aria and M. Gharib, "Reversible tuning of the wettability of carbon nanotube arrays: The effect of ultraviolet/ozone and vacuum pyrolysis treatments," *Langmuir* **27**, 9005–9011 (2011).
- ¹⁵Z. Y. Chen, K. J. Ziegler, J. Shaver, R. H. Hauge, and R. E. Smalley, "Cutting of single-walled carbon nanotubes by ozonolysis," *J. Phys. Chem. B* **110**, 11624–11627 (2006).
- ¹⁶D. B. Mawhinney, V. Naumenko, A. Kuznetsova, J. T. Yates, J. Liu, and R. E. Smalley, "Infrared spectral evidence for the etching of carbon nanotubes: Ozone oxidation at 298 K," *J. Am. Chem. Soc.* **122**, 2383–2384 (2000).
- ¹⁷A. M. Rao, P. C. Eklund, S. Bandow, A. Thess, and R. E. Smalley, "Evidence for charge transfer in doped carbon nanotube bundles from Raman scattering," *Nature* **388**, 257–259 (1997).
- ¹⁸J. M. Simmons, B. M. Nichols, S. E. Baker, M. S. Marcus, O. M. Castellini, C. S. Lee, R. J. Hamers, and M. A. Eriksson, "Effect of ozone oxidation on single-walled carbon nanotubes," *J. Phys. Chem. B* **110**, 7113–7118 (2006).
- ¹⁹M. R. Amer, S. W. Chang, and S. B. Cronin, "Competing photocurrent mechanisms in quasi-metallic carbon nanotube pn devices," *Small* **11**, 3119–3123 (2015).
- ²⁰S. W. Chang, J. Theiss, J. Hazra, M. Aykol, R. Kapadia, and S. B. Cronin, "Photocurrent spectroscopy of exciton and free particle optical transitions in suspended carbon nanotube pn-junctions," *Appl. Phys. Lett.* **107**, 053107 (2015).
- ²¹I. Sarpkaya, E. D. Ahmadi, G. D. Shepard, K. S. Mistry, J. L. Blackburn, and S. Strauf, "Strong acoustic phonon localization in copolymer-wrapped carbon nanotubes," *ACS Nano* **9**, 6383–6393 (2015).

Erratum: “Enhanced photoluminescence in air-suspended carbon nanotubes by oxygen doping” [Appl. Phys. Lett. **109**, 153109 (2016)]

Jihan Chen,¹ Rohan Dhall,¹ Bingya Hou,¹ Sisi Yang,² Bo Wang,² Daejin Kang,³
and Stephen B. Cronin^{1,2}

¹*Ming Hsieh Department of Electrical Engineering, University of Southern California, Los Angeles, California 90089, USA*

²*Department of Physics and Astronomy, University of Southern California, Los Angeles, California 90089, USA*

³*Department of Mechatronics Engineering, Korea Polytechnic University, Shiheung-shi, Gyunggi-do 15073, South Korea*

(Received 12 December 2016; accepted 14 December 2016; published online 3 January 2017)

[<http://dx.doi.org/10.1063/1.4973289>]

The sixth author of this paper¹ is Daejin Kang as shown above.

The authors would also like to acknowledge support from the Northrop Grumman-Institute of Optical Nanomaterials and Nanophotonics (NG-ION²) (B.W).

¹J. Chen, R. Dhall, B. Hou, S. Yang, B. Wang, D. Kang, and S. B. Cronin, “Enhanced photoluminescence in air-suspended carbon nanotubes by oxygen doping,” *Appl. Phys. Lett.* **109**, 153109 (2016).